JOM, Vol. 71, No. 12, 2019
https://doi.org/10.1007/s11837-019-03419-6

The Current Status and Development of Semi-solid Powder Forming (SPF)

XIA LUO,[1,3] MIN WU,[2] CHAO FANG,[1] and BENSHENG HUANG[1]

1.—School of Materials Science and Engineering, Southwest Petroleum University, Chengdu 610500, People's Republic of China. 2.—School of Automobile and Transportation Engineering, Guangdong Polytechnic Normal University, Guangzhou 510635, People's Republic of China. 3.—e-mail: winifreed@163.com

Semi-solid powder forming is a promising near-net-shaped forming technology, which has the advantages of powder metallurgy and semi-solid forming, such as fine grains, low forming pressure and short process flow. It was used to prepare wide solidification range alloys and its composites. Until now, there have been many studies on the parameters, microstructure and mechanical properties of this technology, but few on the forming principles. Because deformation, solidification and densification occur simultaneously, the forming mechanism is very complex. The liquid fraction is the key factor influencing the microstructure and mechanical properties. Semi-solid compression of porous materials was carried out to study the deformation mechanism of semi-solid powders. The combination mechanism and densification process for semi-solid powder rolling has been analyzed, and the compaction behavior of powders in the semi-solid state has been studied. Shima porous yield criterion and Doraivelu plastic yield criterion were applied in the simulation of semi-solid powder rolling. Based on the Fourier heat conduction equation and the related parameters of semi-solid powder, the rolling force and relative density were simulated by using the Marc finite element software platform. The simulation results are in agreement with the experimental results. Although some achievements have been made in the theoretical research and numerical simulation, the yield criteria and mathematical models suitable for semi-solid powder forming need to be further established. In addition, further optimization of this technology and its application in commercial applications should be the research direction.

INTRODUCTION

Semi-solid metal forming (SSF) was first proposed in 1971 by Spencer and co-workers from the Massachusetts Institute of Technology,[1] and attracted much attention because of its special characteristics such as the rheological and thixotropic behaviors. Since then, various shaping and forming processes of mushy, semi-solid or thixo-metals have become popular. Those processes are widely conducted to manufacture the mechanical parts and structural components of passenger cars as well as electronic appliances.[2] A kind of thixo-injection molding technology was utilized to produce the magnesium castings of portable computers and mobile telephones, wheels and driving gears of sport utility bicycles, structure frames of electric hand tools, and components of furniture and housing.[3] However, the customer's requirements for the quality of products are becoming more severe. Higher dimensional accuracy and better surface quality are required with the uniform mechanical property, superior strength, thinner wall thickness, smaller weight, geometrical complexity and functional flexibility. In addition, environmental consciousness as well as excellent productivity and drastic cost reductions are demanded. In order to respond to such requirements, extensive technological improvements of processes, machines, dies and tools are needed. A route based on the premixing and

(Published online March 1, 2019)

compaction of different powders, called semi-solid powder forming (SPF), was developed for the fabrication of metallic slurries.[4]

Figure 1 compares the differences and similarities between SSF and SPF. It can be seen that SPF is the replacement of the bulk material in the SSF into powder materials. Generally speaking, SPF can be divided into four steps: mixing or mechanical alloying, pre-compaction, heating, and forming. In SSF, the preparation of a semi-solid slurry is involved, while it is not required for SPF. Additionally, the microstructure of the material prepared by SPF is also composed of fine equiaxed/near-spherical fine grains. Compared with SSF, SPF has great advantages in preparing particle-reinforced composites,[6] as shown in Table I.

Development History of Semi-solid Powder Forming (SPF)

The development history of SPF is very short and the corresponding studies are limited, and can be dated back to 1986. Yong and Clyne[4] changed the bulk materials to Al-Mg powders for the first time, then heated the mixed powders to a semi-solid temperature range, and injected it into a mold at high speed. Finally, a product with good microstructure was formed and successfully prepared. The product prepared by this method contains nearly spherical grains, which is similar to the microstructure of the materials prepared by SSF. In addition, this technology has also been used to prepare ceramic fiber reinforced materials, which provide a promising way to prepare composites. In 1997, the Musashi Institute used SPF to prepare Al-Si alloys.[7] They heated the mixed powders to a temperature with a 30% volume fraction of liquid, then stirred and injected them into the mold. Finally, materials with excellent microstructure and mechanical properties were obtained. From 2000 to 2006, some researchers used SPF to prepare SiCp, $A1_2O_3$, TiCp and other particle-reinforced aluminum matrix composites.[8–13] The mechanical properties of these prepared samples are higher than those of the composites made by casting. In Ref. 13, three different viscosity equations were first used to simulate the rheological properties and temperature distribution of semi-solid powders. In addition, Wen et al.[14,15] prepared the biomedical titanium alloys (Ti-6Al- and Ti-6Al-4V-based alloys) by SPF, and obtained excellent mechanical properties with different alloying treatments. In 2005, Chen et al.[16] prepared Al-Si alloy by SPF technology, and the silicon particles were fine and uniformly distributed, thus having excellent mechanical properties. However, the above research is still in the primary stage, and there have been few systematic and in-depth analyses of the forming mechanisms. From 2009, Kim and Wu et al.[17–25] used semi-solid powder compaction to prepare aluminum alloys and aluminum matrix composites, adding SiC, carbon nanotubes and graphene as reinforcing materials. The compression behavior, densification process and the rheological properties of semi-solid powders were comprehensively analyzed. In 2011, Liu and Luo et al.[26–34] developed SPF to prepare strips called semi-solid powder rolling, as shown in Fig. 2. They studied the effect of parameters on the microstructure and mechanical properties, densification process, combination mechanisms, rolling force, and deformation mechanisms in detail. In 2018, Wu[35] discussed the crushing methods of semi-solid powders and microstructure transformation, and simulated the density and rolling force distribution during rolling.

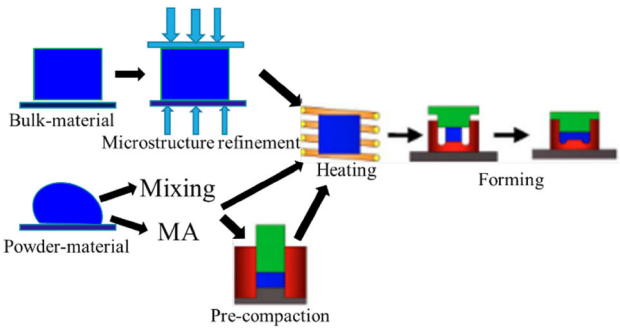

Fig. 1. The preparation between semi-solid forming and semi-solid powder forming. Adapted from Ref. 5.

Further Development of Semi-solid Powder Forming

Thixomolding[36] has come from SSF, and is used to prepare magnesium products. If the raw materials, chips, are replaced by powders, a novel SPF, called semi-solid powder molding, was proposed by the authors (a schematic diagram is shown in Fig. 3). Currently, the authors have prepared medical magnesium alloys with fine microstructures and high properties by this method. The corresponding work will be published soon. In fact, some of the principles of semi-solid powder molding are similar to those of thixomolding, but the microstructure is more homogeneous and the grain size is much smaller. In addition, the excellent microstructure can be obtained without high screw speed and large forces. As shown in Fig. 3, the powders were pre-compacted and put in the mold, and the MgO chips were put on the top layer as a covering agent. Then, pre-compaction was heated to the targeted temperatures and held for a certain time, then consolidated to a dense sample. The related research on thixomolding is relatively mature. The commercial application of magnesium products with a thickness of 0.5–0.6 mm began in 1992.[37] Ghosh and Carnahan,[38–40] and Tsukeda[41] were the earliest authors, but they mainly focused on the study of the organization and mechanical properties. Czerwinski[42–48]

Table I. The characteristics/properties comparison between semi-solid bulk-forming (SSF) and semi-solid powder forming (SPF)

Forming methods	Grain size (μm)	Involved processes	Composites (vol.%)	Strength
SSF	30–50	Solidification/deformation	~ 45	Lower
SPF	20–30	Solidification/deformation/densification	~ 60	Higher

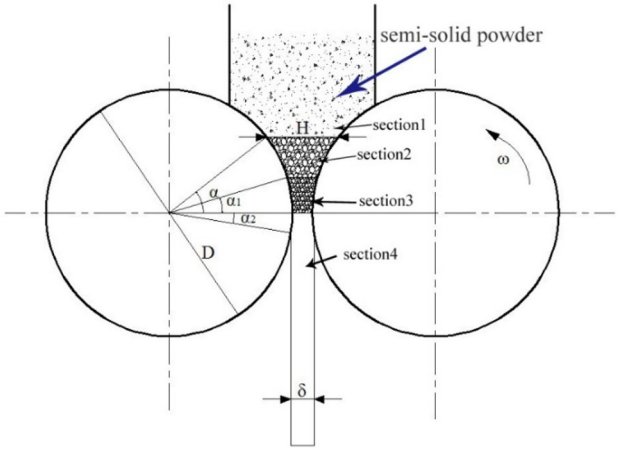

Fig. 2. Schematic of the semi-solid powder rolling process.

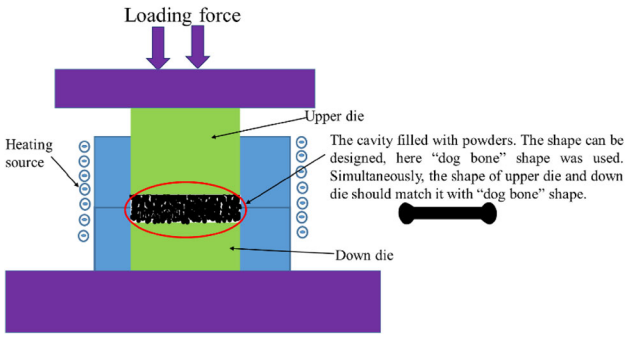

Fig. 3. The schematic diagram of semi-solid powder molding.

carried out a systematic and comprehensive analysis of thixomolding, from the raw materials to the microstructure evolution, and the mechanical properties. Subsequently, the HZG (original name GKSS) magnesium alloy innovation center also carried out related research on thixomolded magnesium alloys.[49,50] The numerical simulation method was used by Jilin University to study thixomolding.[51–54] It was found that the temperature and shear rate are the important factors to determine the viscosity of the semi-solid slurry. The injection velocity affects the shear and filling pressure, but the preheating temperature of the mold has little effect on the microstructure and mechanical properties. From 2010 to 2014, the study of thixomolding gradually changed into the heat treatment process and the thermodynamic properties of magnesium alloys.[55–57] In the whole forming process, there are mainly two aspects determining the performance of the products. The first one is the quality of the semi-solid materials, and the second one is the forming process. However, the quality of the semi-solid alloy materials is much more important. It is possible that using powders not chips can obtain better "semi-solid materials". On the other hand, it can also produce products with thinner walls and a smaller size, which meets the size requirements of biological materials.

SPF technology is still in the primary stage of theoretical research. Most of the studies are still at the stage of the parameter analysis, and microstructure and mechanical properties investigation. The numerical simulation of further forming mechanisms is still in a relatively blank stage. Therefore, there are many problems to be solved. This study summarizes the theoretical foundations, microstructure characteristics, mechanical properties and the development, as well as the current status, of SPF.

THEORETICAL FOUNDATIONS FOR SEMI-SOLID POWDER FORMING

SPF is involved in the deformation, densification and solidification of materials when the liquid and solid phases coexist. However, theoretical studies of the yield criterion and simulation for semi-solid powder forming are rare. The models from many researches on simulation were mainly created based on semi-solid forming or powder forming. Wu and Kim from Iowa State University, and Liu et al. from the South China University of Technology have investigated the forming principles and have created some models to investigate the process principle based on the presented theories.

Theoretical Foundations of Powder Forming

Currently, the numerical simulation of powder forming is mostly carried out by the finite element method, which is mainly based on continuum mechanics. The combination of a powder plasticity mechanics model with the finite element technique has become a hot topic. The Drucker–Prager/Cap model was modified to simulate the rolling process of a Bi-2223/Ag composite strip by the researchers from Tsinghua University.[58] The Shima yield criterion was used to deduce the finite deformation elastoplastic constitutive model for iron and aluminum powder by Liu et al.[59–62] from the South China University of Technology. The slip, movement

and densification process of powder rolling was simulated by using Abaqus software. The relative density of the simulated results agrees well with the experimental results. Chang et al.[63] used the Lagrange–Euler method to simulate the temperature field distribution of iron powder during hot rolling. The powder movement and the relevant mechanical parameters were predicted based on the Shima model. The constitutive equation of the porous materials was proposed by the thermal compression using Deform-3D finite element simulation software.[64–66] Muliadi et al.[67,68] adopted the Drucker–Prager model based on a 2D finite. The bite angle, normal stress, and relative density during powder rolling were calculated based on the Johanson model. The Drucker–Prager yield criterion was used to simulate the gas-driven powder rolling and the relative density distribution. The Shima–Oyane constitutive model was embedded in MSC. Marc to simulate the powder rolling process. Esnault et al.[69] assumed that permeability is a function of material density and particle size, based on Jenike's yield criterion.

Based on the former literature review, it is known that the simulation of powder forming is very complicated. The normal treated way is to regard the powders as a compressible continuum, and then the porous Shima ellipsoidal yield criterion or the Drucker–Prager/Cap yield criterion are used. In fact, the powders are non-continuum.

Theoretical Foundations of Semi-solid Forming

The deformation behavior of semi-solid materials can be divided into two types according to the solid fraction: rheological and viscoplastic.[70] When the solid fraction is below 50%, the semi-solid material is mainly rheological, and is affected by the shear rate and time. The apparent viscosity is usually used to describe the rheological model of semi-solid materials, and is measured by a viscometer or parallel plate compression. When the solid fraction is higher than 50%, the semi-solid material has both rheological and thixotropic properties. The deformation resistance is affected by the semi-solid temperature, strain rate and strain. The stress–strain constitutive relationship of semi-solid materials is the rheology of materials during deformation. The stress of the materials changes with the change of temperature and strain rate. There are two methods to establish the constitutive relationship: the semi-solid compression test and the empirical model.

According to the deformation characteristics of semi-solid materials, the simulation of semi-solid forming can be divided into two methods. One is that the semi-solid material is regarded as a single-phase liquid or a single-phase solid. The other one is that both the solid phase and liquid phase coexist.

Firstly, the semi-solid material is regarded as a non-Newtonian fluid with the solid particles suspended in the liquid. The shear stress is related to the strain rate and the apparent viscosity. The apparent viscosity decreases with the increase of strain rate. The thinning characteristics can be described by the Herschel–Bulkley model, the Ostwald–de-Waele model and the Cross model.[71] The thixoforming process of semi-solid materials was simulated based on the mass conservation continuum equation, energy conservation, and the momentum conservation Navier–Stroke equation. Favier and Atkinson[72–75] and Koeune[76,77] considered the semi-solid materials as a non-Newtonian fluid. The structure coefficients were introduced to describe the characteristics that the semi-solid structure changes with the change of strain and liquid fraction. However, this method ignores the solid phase effect, and it is only suitable for the simulation of the flowing, filling and temperature fields when the liquid fraction is high. In addition, if the semi-solid powders are regarded as liquid phase, the relative density distribution cannot be simulated.

Secondly, the semi-solid material is regarded as a solid phase. The stress–strain constitutive model is used to simulate the forming process. The semi-solid material is treated as a dense material, which meets the Mises yield criterion. The stress–strain constitutive relationship of the semi-solid material is used to describe the deformation characteristics.

Another method is to regard the semi-solid material as a compressible continuous porous material, which satisfies the ellipsoidal yield criterion or the rock yield criterion. The solid fraction represents the relative density of porous material. Many studies treat the semi-solid materials as porous bodies, and the results are in good agreement with the experimental results. This method is also consistent with the characteristic that the discontinuous semi-solid powders are turned into a continuous porous solid, but the action of the liquid phase is ignored.

Thirdly, the semi-solid material is regarded as a solid and liquid coexistence body. The solid phase is treated as a continuous compressible porous body, while the liquid flows in the pores of the solid skeleton. The solid and liquid affect each other and the actions are coupled.[78–82] The stress–strain constitutive model is obtained through the semi-solid compression experiment. The dispersion coefficient is proposed and introduced to the stress–strain constitutive model to describe the solid skeleton fracture effect. Then, the solid phase is regarded as a porous material in accordance with the Shima yield criterion, while the liquid phase is regarded as a Newtonian fluid, and the flowing behavior is consistent with Darcy's law. The Semi-Form S/W program was developed using VB software and the Fortran language based on the above theories. This method takes account of the deformation characteristics of the semi-solid materials. The interaction between the solid and liquid phases is also

considered. Therefore, it better describes the semi-solid forming process. However, for semi-solid powder materials, the existence of discontinuous powders makes it more complicated.

In summary, the simulation of SSF is mainly focused on continuous casting and rolling. The semi-solid material is treated as a single-phase fluid, and then the temperature and rheological fields are simulated. However, SPF is a process of solidification, deformation and densification from semi-solid powders to solid dense materials, so it cannot regard semi-solid powders as a single-phase fluid.

Theoretical Foundations of Semi-solid Powder Forming

For addressing semi-solid metal (SSM), it is normally divided into a solid region and liquid region. At first, the deformation of the solid region (A_S) is implemented as it is assumed to be a porous material, while the liquid region (A_L) is treated as a porosity in the porous material. After the stress (σ_{sij}) acting on the solid region is obtained by assuming that the solid region is a porous material, and then the pressure (p) acting on the liquid region is added to it, the stress (σ_{Tij}) is thus actually acting on the overall SSM (A_T) and represented as follows:[79]

$$\sigma_{Tij}A_T = \sigma_{sij}A_s + \sigma_{ij}pA_L \tag{1}$$

$$\sigma_{Tij} = \sigma_{sij}\frac{A_s}{A_T} + \sigma_{ij}p\frac{A_L}{A_T} = \sigma_{ij} + \sigma_{ij}pf_l. \tag{2}$$

Moreover, the solid fraction (f_s) for the SSM can be equally treated as the relative density, ρ, in a porous material, and the solid fraction is, therefore, defined as follows:

$$f_s = \frac{V_s}{V_s + V_l} = \rho, \tag{3}$$

where V_s is the volume of the solid region and V_l is that of the liquid region. Shima and Oyane's yield criteria[83] for compressible materials are as follows:

$$A = \frac{1}{27}f^2 \quad B = 1, \quad C = f' = f_s^{k'} \tag{4}$$

$$F = \left[3\left(AJ_1^2 + BJ_2'\right)\right]^{\frac{1}{2}} = C\overline{\sigma_0} \tag{5}$$

$$f = \frac{1}{a(1-f_s)^b} \quad k' = 2.5, \quad a = 2.49, \quad b = 0.514, \tag{6}$$

where J_1 is the first invariant of stress, J_2' is the second invariant of deviatoric stress, and $\overline{\sigma_0}$ is the initial stress yield.

As shown in Fig. 4, the pressure applied on the semi-solid powder acts on the solid skeleton and pores at the same time. This figure reflects the deformation and densification process, and the liquid flowing based on the semi-solid compression of the porous material experimental results. The total stress acting on the semi-solid powder is expressed with Eq. 2. However, although Shima and Oyane's model was originally developed for sintered porous metals, the model can be used to predict the behavior of the cold powder compaction process quite successfully.[83] Wu[21] stated that Shima–Oyane model can be used to evaluate the stress required to deform the semi-solid matrix phase when the liquid phase is uniformly distributed in the semi-solid skeleton. The corresponding equation for temperatures between 550°C and 630°C is:

$$f'\sigma_{eq} = \left\{\frac{[\sigma_1-\sigma_2]^2+[\sigma_2-\sigma_3]^2+[\sigma_1-\sigma_3]^2}{2} + \left(\frac{\sigma_m}{f}\right)^2\right\}^{\frac{1}{2}}. \tag{7}$$

If the volume liquid fraction f_l is high (> 30 vol.%), Shima–Oyane's model fails to predict the deformation behavior by some degree.

Wu[35] simulated the semi-solid powder rolling process based on the Shima porous yield criterion and the Doraivelu plastic yield criterion, which is also acceptable when the liquid fraction is higher than 30 vol.%. The rolling process of 2024 aluminum alloy at different temperatures was studied. For the two important parameters of relative density and rolling force, the simulation results are acceptable. Especially when the density is in good agreement with the experimental values, it can provide guidance for the process control and optimization. In this work, it promotes the development of simulation for SPF, and provides some new insights into the corresponding theories.

MICROSTRUCTURES AND MECHANICAL PROPERTIES

As for SSF, the liquid fraction changes the viscosity and deformation resistance, therefore affecting the microstructure and mechanical properties. From these studies,[4–35] it can be seen that the liquid fraction is also the main factor influencing the performance of samples in SPF, because it involves the combination mechanism, densification process, deformation mechanism and solidification. The microstructure of SSF has the feature of rose-shaped grains and near-spherical or equiaxed grains. For SPF, the raw materials are powders, which somehow has the characteristic of spray forming.[84] In order to analyze the microstructure evolution during forming, we should first observe the microstructure of powders in the semi-solid state.

Microstructure of Semi-solid Powder

In order to keep the microstructure of powders in the semi-solid state, the powders were first heated

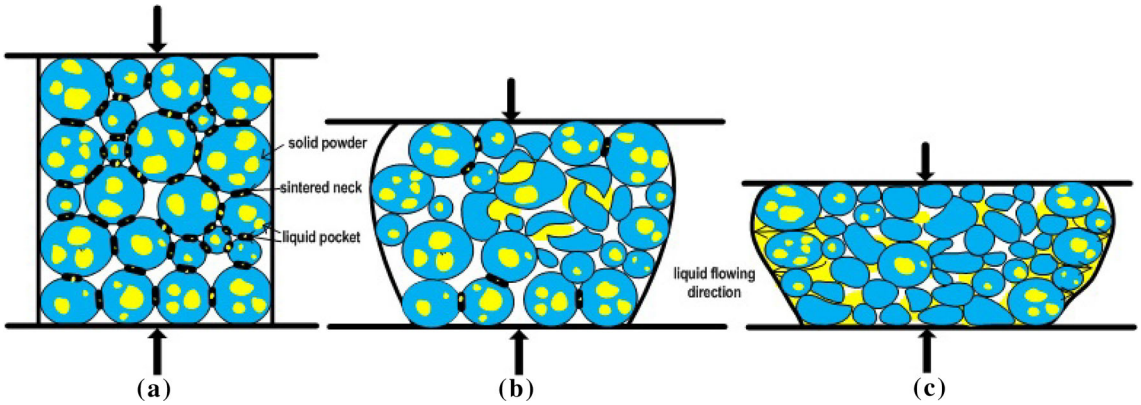

Fig. 4. A schematic diagram of porous materials during semi-solid compression, with the true strain of: (a) 0, (b) 0.22, (c) 0.69.

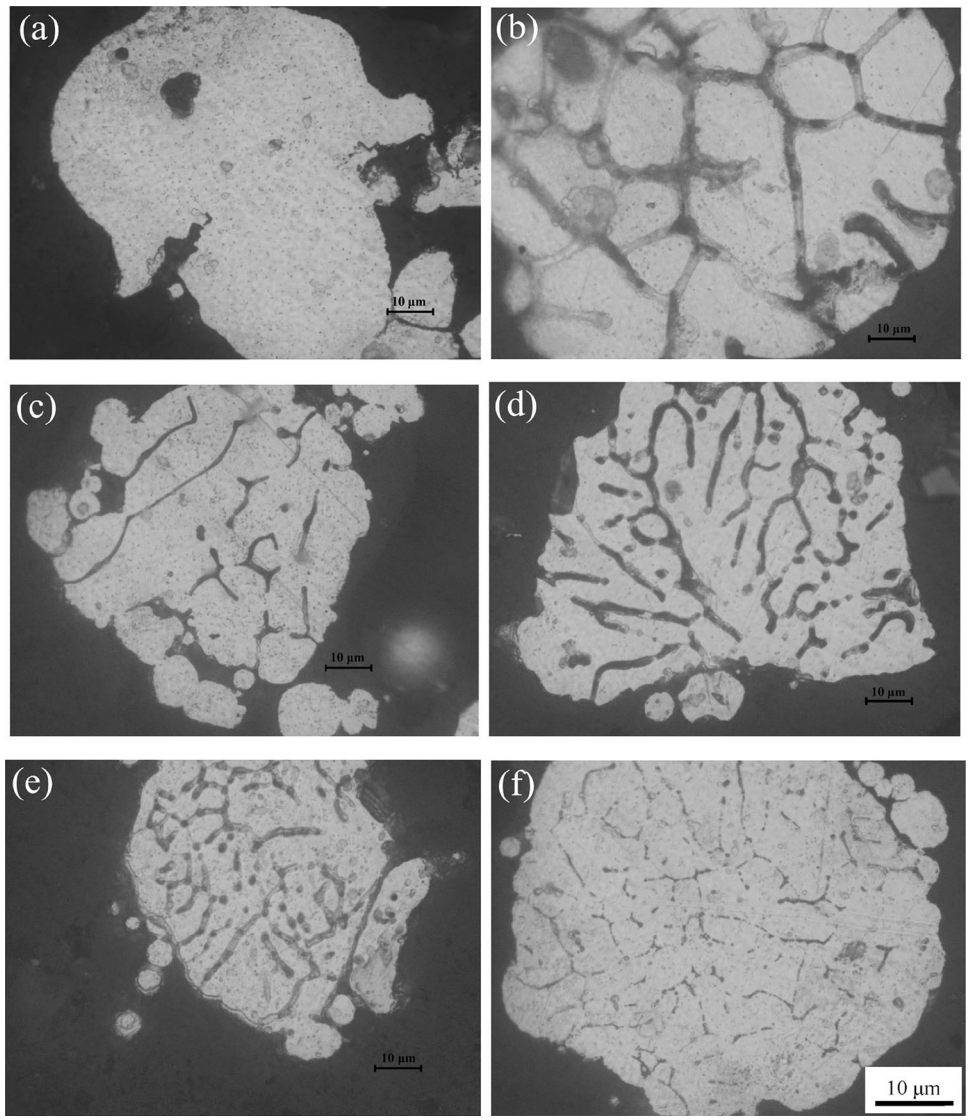

Fig. 5. Microstructures of AA7050 powders prepared under different conditions: heated at 555°C and held for 30 min (a), heated at 585°C and held for 60 min (b), heated at 625°C and held for 60 min (c), heated at 640°C and held for 20 min (d), heated at 650°C and held for 40 min (e), heated at 650°C and held for 50 min (f). Reprinted with permission from Ref. 26.

into the semi-solid temperature range and held for some time in an electric furnace. They were then water-quenched at the selected temperature. As shown in Refs. 21, 26 and 35, an isolated liquid phase first forms within the AA7050 (Fig. 5), 2024 and 6061 powders, and then extends to the particle boundary. As the temperature/liquid fraction increases, some of the liquid phase within the particles may form a network. With the further increase of the liquid, liquid pockets form and result in an irregular solid phase morphology (Fig. 6). In Ref. 33, the changing morphology of AA2024 powders is also the same as that in Ref. 26. It found that the liquid morphology of alloy powders almost follows the pattern of Fig. 5. Wu[35] also discussed the microstructure transformation of AA2024 powder in the semi-solid state, and found that it was similar to a dense material or coarse particles,[48] and equiaxed/granular grains formed during semi-solid insulation. Qstwald ripening can be used to explain the coarsening mechanism, but the coarsening rate is much lower than that of dense material, which may be due to the oxide layer covering the surface of powder, or the pores. Different methods for calculating the liquid fraction of alloy powder have also been discussed, such as the Thermo-Calc method, the DSC method, and the OM method. The final results show that the DSC method is more accurate than the other two methods.

For SPF, it is very important to figure out the liquid morphology, including the location and distribution, because it affects the combination mechanism and flow behavior, which results in the following microstructure and mechanical properties of the samples.

Microstructure and Mechanical Properties

In almost all of these studies related to SPF, their results indicate that this method provides a promising method to obtain fine and homogenous microstructures with equiaxed grains. Additionally, it shows a potential in the preparation of reinforced composites with a high volume fraction of reinforced particles, and because it combines semi-solid forming and powder metallurgy, it is very easy to obtain microstructures with those features.

As shown in Fig. 7, the semi-solid powder rolled 2024 aluminum alloy consists of fine grains with few spherical grains in the microstructures, which somehow has the features of semi-solid forming; however, fine dendrites were also observed. With the increase of rolling temperature, the porosity and grain size of the strip gradually decreases. The spherical particles change into equiaxed fine grains, then grow up to the long grains when the rolling temperature keeps increasing. Obvious cracks and grain coarsening occur when rolled at 610°C. The relative density of s the trips increases with the increase of temperature, while it decreases slightly at 610°C. Therefore, the optimum rolling temperature of the 2024 aluminum alloy is 600°C, which is consistent with the results of the semi-solid compression of porous materials.[33]

Figure 8 shows the microstructure of semi-solid powder rolled AA7050 strips, and the corresponding relative density is shown in Fig. 9. When prepared at low temperature, the microstructure is characterized by a randomly distributed rosette structure with isolated pores and some deformed or broken powder particles. The relative density (87.1%) and micro-hardness (77.32 HV) are both low. The original particle boundaries and most pores disappear prepared at 585°C, and its microhardness and relative density just increase slightly. Those microstructures of strips prepared at the liquid fraction ranging from 45% to 65% are characterized by a few rosettes, some dendrite grains and fine equiaxed grains, without original powder boundaries. The microhardness dramatically increases to 161.6 HV when the liquid fraction reaches 45%, and then reaches the peak when the liquid fraction is 65%. If the liquid fraction keeps increasing (to 85%), the strips consist of flaws and coarse rosette-structure grains (Fig. 8e and f). The microhardness and relative density also decrease fractionally.

From Kim and Wu's studies,[17–25] the microstructure of semi-solid powder-extruded samples also consists of fine and spherical grains. With the increase of temperature or liquid fraction, many powder boundaries disappear and metallurgical bonding occurs, while grain size become finer and relative density increases. However, too much liquid

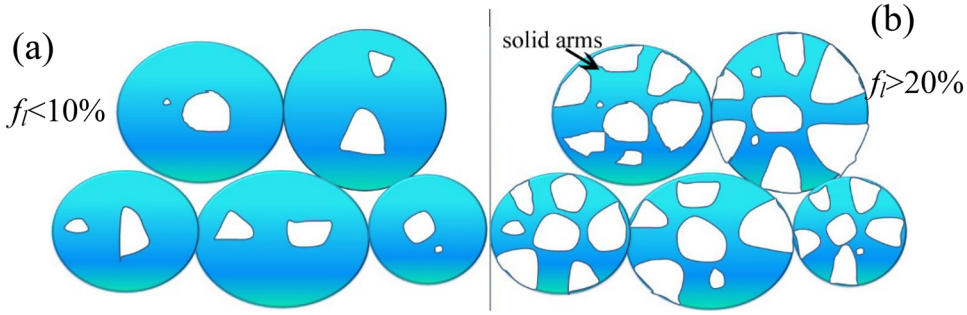

Fig. 6. Illustration of the semi-solid powder morphology in powder forming: $f_l < 10\%$ (a), $f_l > 20\%$ (b). Reprinted with permission from Ref. 28.

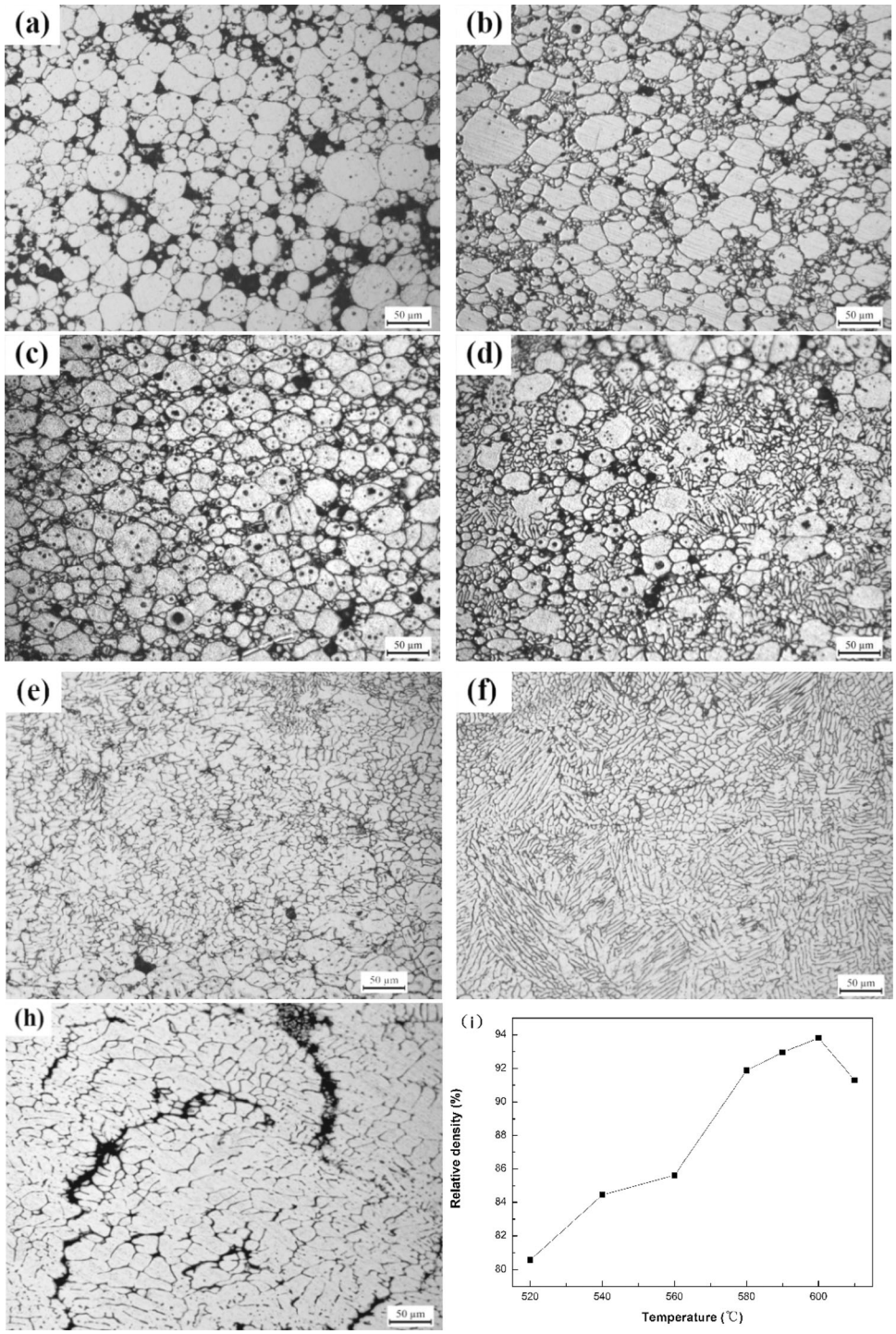

Fig. 7. The microstructure and relative density of 2024 aluminum alloy powders rolled at different semi-solid temperatures: (a) 520°C; (b) 540°C; (c) 560°C; (d) 580°C; (e) 590°C; (f) 600°C; (h) 610°C; (i) the relative densities at different temperatures. Reprinted with permission from Ref. 35.

makes the grains coarse with more flaws or cracks. It can be seen that the microstructure of semi-solid powder-processed samples is greatly affected by the liquid fraction, and their changing trend stays nearly the same. The liquid somehow plays the role of binder between powders, which makes the metallurgical bonding occur. The combination mechanism among powders is different with different liquid fractions.[26] In SPF, solidification, densification and deformation occur simultaneously, and the action of liquid is different from that of SSF. Therefore, some principles of SSF cannot be directly applied in SPF. The microstructure evolution, combination mechanism, densification process and deformation behavior have been investigated in detail.

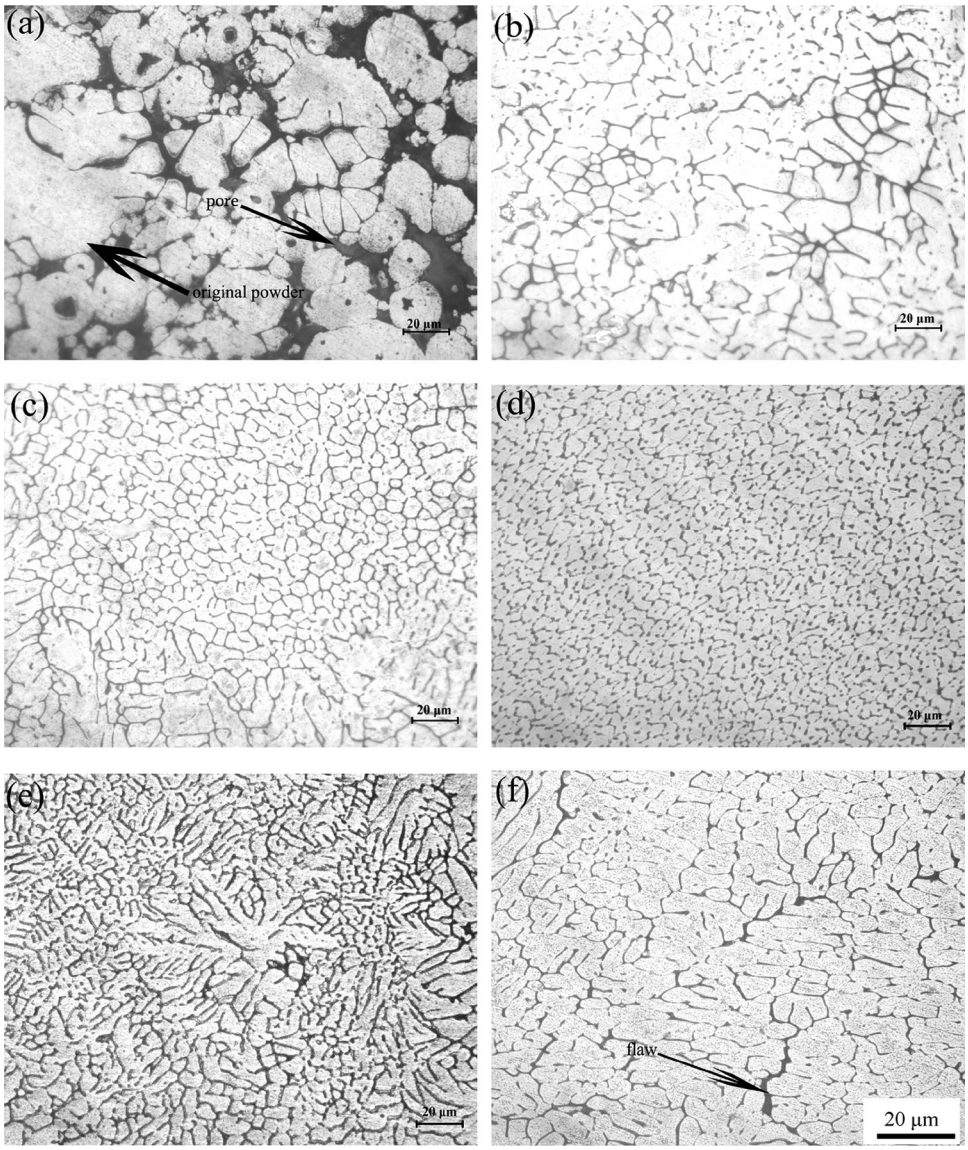

Fig. 8. Microstructures of strips prepared under different conditions: heated at 555°C and held for 30 min (a), heated at 585°C and held for 60 min (b), heated at 625°C and held for 60 min (c), heated at 640°C and held for 20 min (d), heated at 650°C and held for 40 min (e), heated at 650°C and held for 50 min (f). Reprinted with permission from Ref. 26.

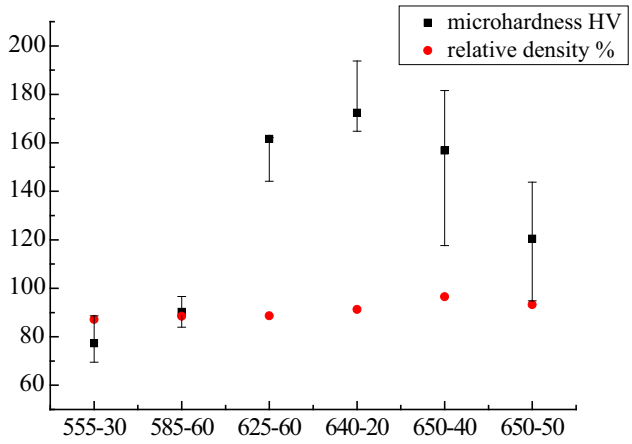

Fig. 9. Relative density and microhardness of strips prepared under different conditions. Reprinted with permission from Ref. 26.

Additionally, the effect of particle size on the microstructure and mechanical properties was analyzed,[31] and the tensile properties are shown in Table II. From the results, particle size influences the tensile strength greatly. As the powder size increases, more liquid was squeezed out at the same rolling temperature. Both the relative density and rolling force increase with the increase of powder size. Seen from these results, coarse powders have a better flow property, which is consistent with solid powder forming. Actually, it is very easy to understand from thixomolding of magnesium alloys,[36] because the raw materials in thixomolding are chip or coarse powders, while it is fine powder in SPF. If the powder size reaches to a high level, the powders can be regarded as chip, when it turns into thixomolding. Thus, semi-solid powder moulding has

Table II. Tensile properties of semi-solid powder rolled strips after heat treatment. Reprinted with permission from Ref. 31

Materials	Ultimate tensile strength (MPa)	Yield strength (MPa)	Elongation at failure (%)
528°C–30 min (270 μm)	444 ± 18	400 ± 7	6.9 ± 1.6
555°C–30 min (270 μm)	439 ± 14	391 ± 4	8.3 ± 1.0
585°C–30 min (270 μm)	390 ± 4	382 ± 1	9.6 ± 0.3
625°C–30 min (270 μm)	352 ± 21	332 ± 19	8.8 ± 2.1
625°C–30 min (147 μm)	382 ± 1	367 ± 1	10.9 ± 0.1
625°C–30 min (104 μm)	383 ± 4	326 ± 4	12.8 ± 0.2

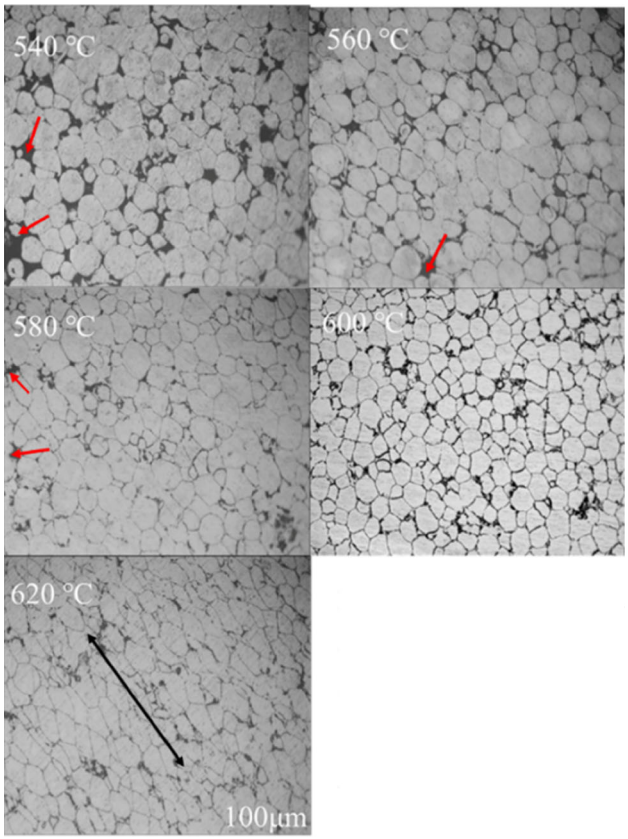

Fig. 10. Microstructures of semi-solid powder molding Mg-3Zn alloy prepared at different temperatures.

Table III. Relative densities of Mg-3Zn prepared at different temperatures

Temperature (°C)	540	560	580	600	620
Relative density (%)	83.4	86.1	87.0	97.4	91.4

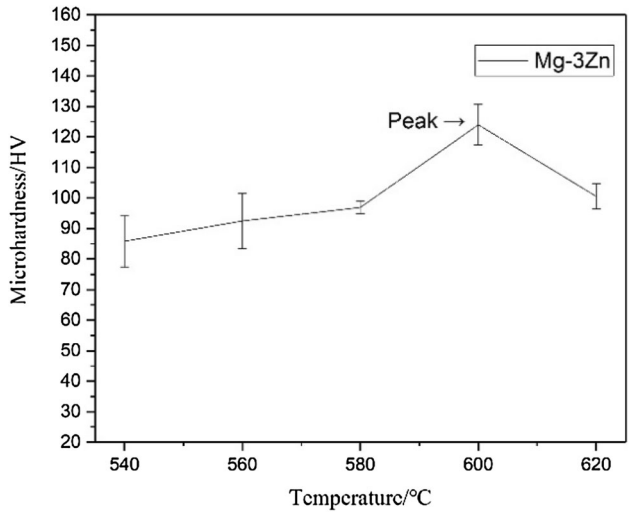

Fig. 11. Microhardness of Mg-3Zn alloy prepared at different temperatures.

been proposed by the authors, which combines powder forming and thixomolding. Currently, it has been used to successfully prepare a medical Mg-3Zn alloy. The effect of powder geometry on the forming process will also be taken into consideration.

Figure 10 shows the microstructure of the Mg-3Zn alloy prepared at 540°C, 560°C, 580°C, 600°C, and 620°C. With the temperature increases, the pores becomes fewer (the red arrows show the pores). At the start, the particle boundaries and pores are clearly observed, while some original powders still keep their morphology. The corresponding relative density is not very high, with the corresponding value of 83.4% (shown in Table III). As the temperature increases, the pores are gradually eliminated and the particles/powders are deformed, while more metallurgical bonds occur. At the same time, their relative densities slowly increase from 86.1% to 87%. When the temperature increases to 600°C (Fig. 10), fine equiaxed grains are observed and most of the pores disappear. The relative density dramatically reaches to the highest value of 97.4%. If the temperature further increases, the grains are elongated perpendicular to the extrusion direction (as shown by the arrows in Fig. 10). A little of the liquid is squeezed out, and the relative density decreases to 91.4%.

Figure 11 shows the microhardness of the Mg-3Zn alloy prepared at different temperatures, and the changing trend with the temperature increasing. As the injection temperature increases, the microhardness also increases, which is consistent

with that of the relative density. When the temperature is 600°C, the microhardness reaches to its highest value (125 HV). If the temperature keeps increasing, then the microhardness decreases. Figure 12 shows the compressive stress of the Mg-3Zn alloy prepared at different temperatures. When the temperature is lower than 600°C, compressive stress changes little staying at close to 300 MPa. It also reaches a high value of 315 MPa at 600°C. The mechanical properties, including microhardness and compressive stress, are higher than that of Mg-Zn alloys prepared by casting.[85] The fine grains also contribute to high microhardness and compressive stress.

Seen from the microstructure and mechanical properties, liquid is also the key factor affected by the temperature. With the increase of temperature, the grain size become finer, pores and particle boundaries disappear, and the relative density and the strength reach their highest values. If the temperature increases further, the microstructure and mechanical properties become poor. Their changing trend also follows that of semi-solid powder rolling or semi-solid powder extrusion.

THE CURRENT DEVELOPMENT AND THE FUTURE

SPF technology can prepare homogeneous microstructures with fine grains, with improvement of the mechanical properties for the finished products, which can then be used to mix different types and contents of reinforced particles. It has great advantages in the preparation of composite materials, and is a very promising near-net-forming method. Currently, it is mainly used to prepare aluminum alloys and composites. The application of other material systems has been gradually increasing in recent years, such as in medical Mg-based alloys.

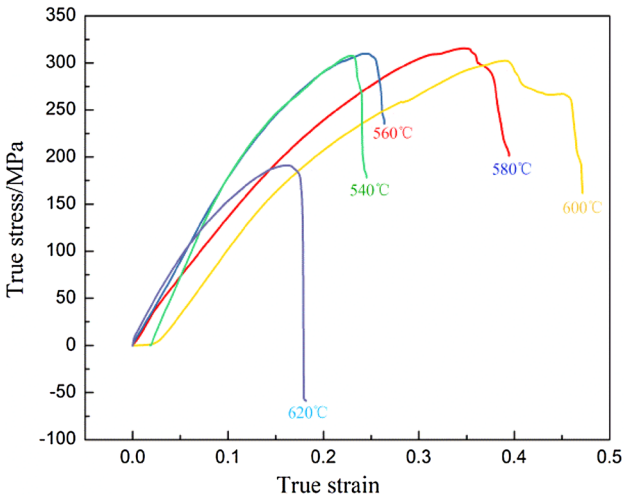

Fig. 12. Compressive stress–strain curves of Mg-3Zn alloy prepared at different temperatures.

Generally, research on SPF is mostly focused on the parameters of the combination mechanism, densification, solidification and so on. Theoretical studies such as numerical simulation are rarely reported. Until now, SPF has attracted some attention, and has been used to prepare tool steel, titanium alloys, aluminum alloys and other materials and composites, with improved mechanical properties. However, the above research is still in the preliminary experimental stage, and there are few systematic and comprehensive studies on the forming mechanism. Wu[35] studied the crushing methods of semi-solid powders and numerical simulation based on the theories of powder forming and semi-solid forming. The simulated results, Fig. 13 (the temperature and relative density distribution of strips during semi-solid powder rolling), and Fig. 14 (the rolling force at different stages; the results obtained at 580°C), are basically in agreement with the experimental results. These take the theoretical study a big step forward.

In the next step, the following work are intended to be carried out:

1. Observation of the forming process, liquid flow among the powders or in the pores, together with powders or debris, contributing to the deformation and densification. However, the flow behavior, dynamics and mathematical model of liquid are still unclear, and need further investigation. Additionally, the liquid flow is not considered in the simulation of semi-solid powder rolling at higher processing temperatures. It is hoped that the effect of liquid flow can be introduced into the simulation process by changing the algorithm, so as to be closer to the actual forming process. Based on the results from Karagadde and Lee,[86] a synchrotron is a fantastic method to achieve this.
2. The difference between holding time and powder size cannot be simulated because the specific

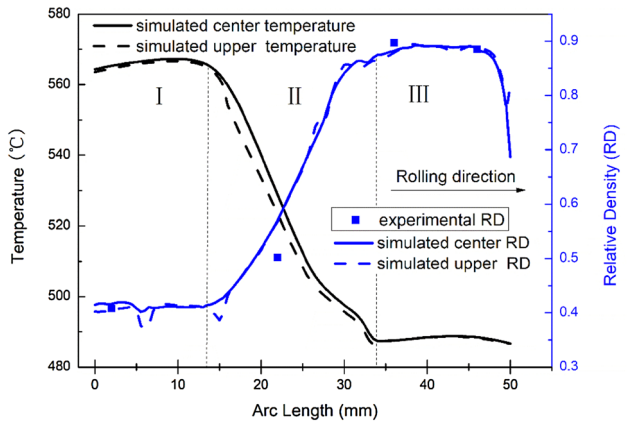

Fig. 13. Comparison of the relative density and temperature (obtained by simulation and experiments) at the surface and center of strips along the rolling direction. Reprinted with permission from Ref. 35.

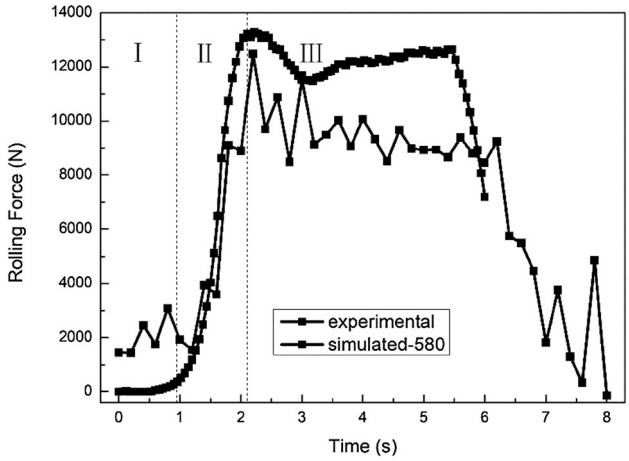

Fig. 14. Comparison of the rolling force (obtained by simulation and experiments). Reprinted with permission from Ref. 35.

deformation resistance is uncontrollable. It is hoped that a constitutive equation related to holding time and particle size can be established to refine the simulation of semi-solid powder forming.

3. The yield criterion and theoretical models for semi-solid powders are intended to be created based on the former results. On the other hand, this near-net-shape forming should be further optimized and then applied in industrial areas.

ACKNOWLEDGEMENTS

The authors gratefully acknowledge the financial support of the Young Scholars Development Fund of SWPU (No. 201599010066), National Natural Science Foundation of China (No. 51704255), and Open Fund of National Engineering Research Center of Near-net-shape Forming Technology for Metallic Materials, South China University of Technology (No. 2015002).

REFERENCES

1. D.B. Spencer, R. Mehrabian, and M.C. Flemings, *Metall. Trans.* 3, 1925 (1972).
2. M. Kiuchi and R. Kopp, *CIRP Ann. Manuf. Technol.* 51, 653 (2002).
3. D. Walukas, S. Labeau, N. Prewitt, and R. Decker, *Mater. Technol.* 109, 1 (2000).
4. R.M.K. Yong and T.W. Clyne, *J. Mater. Sci.* 21, 1057 (1986).
5. Y.F. Wu, *Development of Novel Semisolid Powder Processing for Micro-Manufacturing*, Graduate Theses and Dissertations, Paper 10568 (2009).
6. T.J. Chen, H. Qin, and X.Z. Zhang, *J. Mater. Sci.* 53, 2576 (2018).
7. T. Marooka, *Met. Powder Rep.* 52, 39 (1997).
8. S.J. Luo and L.J. Zu, *Trans. Nonferrous Met. Soc. China* 10, 304 (2000).
9. L.J. Zu, S.J. Luo, and H.Y. Zhang, *J. Harbin Inst. Technol.* 32, 69 (2000) **(in Chinese)**.
10. L.J. Zu and S.J. Luo, *Trans. Nonferrous Met. Soc. China* 10, 179 (2000) **(in Chinese)**.
11. L.J. Zu and S.J. Luo, *J. Mater. Proc. Technol.* 114, 189 (2001).
12. S.J. Luo, Y.S. Cheng, and P.X. Wang, *Trans. Nonferrous Met. Soc. China* 16, 772 (2006).
13. R.W. Hamilton, Z. Zhu, R.J. Dashwood, and P.D. Lee, *Compos. A* 34, 333 (2003).
14. K. Yasue, G.L. Yu, C.E. Wen, and Y. Yamada, *J. Mater. Sci.* 35, 5927 (2000).
15. C.E. Wen, K. Yasue, and Y. Yamada, *J. Mater. Sci.* 36, 1741 (2001).
16. C.M. Chen, C.C. Yang, and C.G. Chao, *J. Mater. Proc. Technol.* 167, 103 (2005).
17. Y. F. Wu, G.Y. Kim, I.E. Anderson, and T. Lograsso, Fabrication of graded structure in SiC-reinforced metal matrix by semisolid powder processing, *Proceedings of the ASME 2009 International Manufacturing Science and Engineering Conference. USA, West Lafayette, Indiana*, vol. 10 (2009), p. 4.
18. Y.F. Wu, G.Y. Kim, I.E. Anderson, and T. Lograsso, *J. Manuf. Sci. Eng.* 132, 0110031 (2010).
19. Y.F. Wu, G.Y. Kim, I.E. Anderson, and T. Lograsso, *Acta Mater.* 58, 4398 (2010).
20. Y.F. Wu and G.Y. Kim, *J. Mater. Proc. Technol.* 211, 1341 (2011).
21. Y.F. Wu and G.Y. Kim, *Powder Technol.* 214, 252 (2011).
22. Y.F. Wu, *Fabrication of Metal Matrix Composite by Semi-Solid Powder Processing* (Ames: Iowa State University, 2011).
23. Y.F. Wu, G.Y. Kim, and A.M. Russell, *Mater. Sci. Eng. A* 532, 558 (2012).
24. Y.F. Wu, G.Y. Kim, and A.M. Russell, *Mater. Sci. Eng. A* 538, 164 (2012).
25. M. Bastwros, G.Y. Kim, C. Zhu, K. Zhang, S.R. Wang, X.D. Tang, and X.W. Wang, *Compos. B* 60, 111 (2014).
26. Y.Z. Liu, X. Luo, and Z.L. Li, *J. Mater. Proc. Technol.* 214, 165 (2014).
27. X. Luo, Y.Z. Liu, C.X. Gu, and Z.L. Li, *Powder Technol.* 216, 161 (2014).
28. X. Luo, Y.Z. Liu, Z.Q. Mo, and C.X. Gu, *Metall. Mater. Trans. A* 46A, 2185 (2015).
29. X. Luo, Y.Z. Liu, and H.F. Jia, *Oxid. Met.* 83, 55 (2015).
30. X. Luo, *Study on the Process and Principle of Semi-solid Powder Rolling for Preparation of 7050 Aluminum Strip*, South China University of Technology, Doctoral thesis (2015) **(in Chinese)**.
31. X. Luo and Y.Z. Liu, *JOM* 68, 3078 (2016).
32. Z.Q. Mo, Y.Z. Liu, H.F. Jia, and M. Wu, *Trans. Nonferrous Met. Soc. China* 25, 3181 (2015).
33. W. Min, Y.Z. Liu, T. Wang, and K.B. Yu, *Mater. Sci. Eng. A* 674, 144 (2016).
34. W. Min, Y.Z. Liu, Z. Zeng, and W.Y. Luo, *JOM* 69, 763 (2017).
35. M. Wu, *Process Principles and Numerical Simulation on Semi-Solid Powder Forming and Porous Materials Deformation of 2024 Aluminum Alloy*. South China University of Technology, Doctoral thesis (2018) **(in Chinese)**.
36. Y.F. Zhang, *Microstructure and Properties of Thixomolding Magnesium Alloy and Simulation of Forming Process*. Jilin University, Doctoral thesis (2008) **(in Chinese)**.
37. J.L. Tang and D.B. Zeng, *Foundry Equip. Technol. China* 6, 3 (2000) **(in Chinese)**.
38. D. Ghosh, K. Kang, C. Bach, et al., Properties and microstructure of thixomolded and heat treated AZ61A magnesium alloy.*Advanced in Production and Fabrication of Light Metals and Metal Matrix Composites*, ed. M.M. Avedesian, L.J. Larouehe, and J. Masounave (Montreal: The Metallurgical Society of the CIM, 1992), p. 399.
39. B. Mansoor, S. Mukherjee, and A. Ghosh, *Mater. Sci. Eng. A* 512, 10 (2009).
40. R.D. Carnahan, R. Hathaway, and R. Kilbert, Thixomolded AZ91D magnesium: mechanical and microstructural property dependency on process parameter variations. *Proceedings of the International Symposium on Light metals Processing and Applications, Quebec City, PQ* (1993), p. 325.
41. T. Tsukeda, K. Takeya, K. Saito, et al., *J. Jpn. Inst. Light Met.* 49, 287 (1999).
42. F. Czerwinski, P.J. Pinet, and J. Overbeeke, *The Influence of Primary Solid Content on the Tensile Properties of a*

Thixomolded AZ91D Magnesium Alloy, Magnesium Technology 2001 of TMS (New Orleans, LA: The Minerals, Metals & Materials Society, 2001), p. 99.
43. F. Czerwinski, A. Zielinska, P.J. Pinet, and J. Overbeeke, *Acta Mater.* 49, 1225 (2001).
44. F. Czerwinski, *Acta Mater.* 50, 3265 (2002).
45. F. Czerwinski, *Scr. Mater.* 48, 327 (2003).
46. F. Czerwinski, *Acta Mater.* 52, 5057 (2004).
47. F. Czerwinski, *Acta Mater.* 53, 1973 (2005).
48. F. Czerwinski, *Metall. Mater. Trans. B* 1, 3320 (2018).
49. M. Scharrer, A. Lohmüller, R.M. Hilbinger, et al., Advances in Magnesium Injection Molding (Thixomolding®). *Proceedings of the 7th International Conference Magnesium Alloys and Their Applications, Dresden* (2006).
50. H. Frank, N. Hort, H. Dieringa, and K.-U. Kainer, *Solid State Phenom.* 141–143, 43 (2008).
51. W. Liang, Y.B. Liu, X.P. Cui, et al., *Automot. Technol. Mater.* 15, 15 (2004) **(in Chinese)**.
52. Y.F. Zhang, Y.B. Liu, Z.Y. Cao, L. Zhang, and Q.Q. Zhang, *Trans. Nonferr. Met. Soc. China* 18, 703 (2008) **(in Chinese)**.
53. Y.F. Zhang, Y.B. Liu, Q.Q. Zhang, Z.Y. Cao, X.P. Cui, and Y. Wang, *Mater. Sci. Eng. A* 444, 251 (2007).
54. X.P. Cui, H.Y. Xu, H.F. Liu, T. Zhang, and Y.B. Liu, *Adv. Mater. Res.* 503–504, 90 (2012).
55. H.A. Patel, D.L. Chen, S.D. Bhole, and K. Sadayappan, *J. Alloys Compd.* 496, 140 (2010).
56. L.J. Yang, Y.H. Wei, and L.F. Hou, *J. Mater. Sci.* 45, 3626 (2010).
57. T.D. Berman, *Microstructure Evolution and Tensile Deformation in Mg Alloy AZ61 through Thixomolding and Thermomechanical Processing*. University of Michigan, Doctoral thesis (2014).
58. L.P. Lei, Y.H. Zhao, and P. Zeng, *Supercond. Sci. Technol.* 18, 818 (2005) **(in Chinese)**.
59. M.J. Liu, W. Xia, and Z.Y. Zhou, *Mach. Design Manuf.* 532–533, 817 (2006) **(in Chinese)**.
60. Z.X. Zheng Experimental and Numerical modeling for powder rolling. *International Conference on Physical and Numerical Simulation of Materials Processing* (2010), p. 115.
61. C. Qiu, Z.X. Zheng, W. Xia, and Z.Y. Zhou, *Adv. Mater. Res.* 211–212, 1182 (2011).
62. M.J. Liu and G.C. Liu, *Adv. Mater. Res.* 569, 111 (2012).
63. H.J. Chang, H.N. Han, and S.H. Joo, *Int. J. Mach. Tools Manuf.* 47, 1573 (2007).
64. A. Michrafy, H. Diarra, J.A. Dodds, and M. Michrafy, *Powder Technol.* 206, 154 (2011).
65. A. Michrafy, H. Diarra, J.A. Dodds, M. Michrafy, and L. Penazzi, *Powder Technol.* 208, 417 (2011).
66. H.B. Li, *Finite Element Simulation and Experimental Study on Rolling Process of Powder Metallurgy Molybdenum Plate* (Taiyuan: Taiyuan University of Technology, 2011) **(in Chinese)**.
67. A.R. Muliadi, J.D. Litster, and C.R. Wassgren, *Powder Technol.* 221, 90 (2012).
68. A.R. Muliadi, J.D. Litster, and C.R. Wassgren, *Powder Technol.* 237, 386 (2013).
69. V. Esnault, A. Michrafy, D. Heitzmann, M. Michrafy, and D. Oulahna, *Powder Technol.* 270, 484 (2015).
70. H.V. Atkinson, *Cheminform* 36, 341 (2005).
71. J. Chowdhury, S. Ganguly, and S. Chakraborty, *J. Phys D* 38, 2869 (2005).
72. V. Favier and H. Atkinson, *Trans. Nonferrous Met. Soc. China* 20, 1691 (2010).
73. V. Favier and H.V. Atkinson, *Acta Mater.* 59, 1271 (2011).
74. A. Neag, V. Favier, R. Bigot, and H.V. Atkinson, *J. Mater. Proc. Technol.* 229, 338 (2016).
75. V. Favier, P. Cézard, and R. Bigot, *Mater. Sci. Eng. A* 517, 8 (2009).
76. R. Koeune and J.P. Ponthot, *Int. J. Plastic.* 58, 120 (2014).
77. R. Koeune and J.P. Ponthot, *J. Comput. Appl. Math.* 234, 2287 (2008).
78. C.G. Kang and J.H. Yoon, *J. Mater. Proc. Technol.* 66, 76 (1997).
79. C.G. Kang and H.K. Jung, *Int. J. Mech. Sci.* 41, 1423 (1999).
80. J.H. Hwang, D.C. Ko, and G.S. Min, *Int. J. Mach. Tools Manuf.* 40, 1311 (2000).
81. D.C. Ko, G.S. Min, B.M. Kim, and J.C. Choi, *J. Mater. Proc. Technol.* 100, 95 (2000).
82. C.G. Kang, P.K. Seo, and M.D. Lim, *Int. J. Mech. Sci.* 45, 1949 (2003).
83. S. Shima and M. Oyane, *Int. J. Mech. Sci.* 18, 285 (1976).
84. K. Raju, S.N. Ojha, and A.P. Harsha, *J. Mater. Sci.* 43, 2509 (2008).
85. Y.Z. Du, B.L. Jiang, and Y.F. Ge, *Vacuum* 148, 27 (2018).
86. S. Karagadde, P.D. Lee, B. Cai, J.L. Fife, M.A. Azeem, K.M. Kareh, C. Puncreobutr, D. Tsivoulas, T. Connolley, and R.C. Atwood, *Nat. Commun.* 6, 8300 (2015). https://doi.org/10.1038/ncomms9300.